
Chemistry Europe
Excellence in Chemistry Research Worldwide
Front Cover:
Photo by Rodion Kutsaiev on Unsplash
journal.chemistry-europe.org
WILEY-VCH

ChemistrySelect

Research Article
doi.org/10.1002/slct.202204249

Chemistry Europe
European Chemical Societies Publishing

www.chemistryselect.org

Surface and Structural Modulation of Waste-Derived, Boron-Doped Carbon to Enhance its Adsorption Efficiency for Lead Removal from Wastewater

Hafiz Muhammad Aamir,*[a] Matthew L Alexander,*[a] and Tanveer ul Haq[b]

Lead is a common hazardous heavy metal found in agricultural soil and industrial wastewater. It is a dire need for society to remove lead from wastewater via a facile and cost-effective route, which is needed to improve water quality. Here we obtain boron (B) doped porous carbon (BC) via two-step thermal pyrolysis of waste tires, as it is a promising raw material. The B doping changes the coordination chemistry, physicochemical properties, and surface structure of carbon. The degree of graphitization, boron content, and pore size distribution of BC was controlled by thermal treatment and $NaBH_4$ content. The surface topography, elemental composition, degree of graphitization, chemical structure, and lead (Pb) removal efficiency of BC was thoroughly analyzed by SEM, EDS, Raman, XRD, XPS, and ICP-OES analysis. Benefiting from the structural disorder, high specific surface area, and least coordinated exposed carbon, the BC revealed high adsorption efficiency (98.02 %) for lead removal from wastewater.

Introduction

Lead is a dangerous material if not used properly and can cause anemia, kidney malfunction, tissue damage to the brain, and even death in extreme situations. Lead is found in all living organisms and in the earth's crust (50 ppm) and seawater (5 ppb). The human body contains 121 ppb, 96 % of it being found in bone. As the human body ages, the lead may reach a limit of 400 mg. While lead may help enhance protein synthesis, DNA synthesis, and cell replication, it is not an essential element for mammals. If the human body has a significant lead intake, about 800 mg, it may cause significant problems, as discussed earlier. The presence of lead in any water, especially wastewater, is hazardous as it will harm not only humans but also aquatic life and flora, even in small concentrations. Most of this lead in wastewater comes from process industries requiring lead in materials, for example, paint, oils, lead-acid batteries, fertilizer, etc.[1–3] An excess amount of lead will cause harm to both mammals and sea life. It is a dire need for society to mitigate lead usage such that the recommended amount of 0.05 mg/L is not exceeded in water. An even more stringent regulatory level of 0.02 mg/L in water has been proposed and is under review by the EPA.[4] Several chemical and physicochemical methods for treating wastewater containing lead wastes are known, such as chemical precipitation, electrochemical reduction, ion exchange, biosorption, and adsorption.[5–9] The choice of treating lead depends on many factors, such as the pH of the water, temperature, flow volume, etc. However, the most common treatment method is the adsorption of lead using activated carbon, a black solid substance resembling crushed charcoal.[10–12] While this method works well, activated carbon is expensive, and research on low-cost alternatives has grown. In this study, we pyrolyzed waste tires, as their low ash content and excellent structure make them suitable for preparing microporous activated carbon.

Activated carbon is considered a promising material for metal adsorbents due to its multilevel porosity and high internal specific surface area.[13] Its high mechanical strength endorsed its practical viability for heavy metal removal in harsh conditions. Recently, researchers widely employed these carbon-based materials in catalysis, gas treatment, and as adsorbents for wastewater treatment.[14,15] Carbon-based materials' high demand and affordability have triggered substantial attention in the search for inexpensive carbon-based adsorbents, mainly derived from waste with the same physicochemical properties.[16] This approach is cost-effective and overcomes disposal challenges. The most common approach for carbon derivation from waste is high-temperature pyrolysis, followed by chemical activation.[17,18] The pyrolysis process determines the carbon contents, i.e., graphitized carbon, pyrrolic, and pyridinic carbon, and creates the surface porosity that provides the short diffusion channels for mass migrations, while the chemical activation increases the porosity and controls the pore size distribution.[19] Different carbon precursors need harsh physical and chemical conditions for activation, limiting its range for adsorption of different chemical species. The need is to derive carbon from waste via a cost-effective, scalable, and environmentally benign process that results in high porosity and high specific surface area.

It is well established that heteroatom doped porous carbon has unique features of active sites with controlled chemical environment that enriches heavy metal presence around the active/adsorption site and intensifies the adsorption capacity of

---

[a] H. M. Aamir, Dr. M. L Alexander
Department of Chemical & Natural Gas Engineering, Frank H. Dotterweich College of Engineering, Texas A&M University-Kingsville, TX, Kingsville 78363-8202, USA
E-mail: hafiz_muhammad.aamir@students.tamuk.edu
matthew.l.alexander@leidos.com
[b] Dr. T. ul Haq
Department of Chemistry, College of Sciences, University of Sharjah, P.O. Box 27272, Sharjah, N/A UAE

carbon-based materials.[20] The heteroatom doping reshuffles the electronic density around carbon active centers, creates abundant active sites with intrinsic adsorption capability, and activates the carbon framework.[21] The heteroatom doping causes the defect enrichment that additionally provides the adsorption site for heavy metal removal.[22]

A low-energy and extremely quick method for producing N,S-co-doped carbon from ternary deep eutectic solvents was described by Cai and workers.[22] In comparison to single-doped carbon (396.2 mg/g) and pristine carbon (186.4 mg/g), the N, S-co-doped carbon's adsorption capacity for Cr(VI) dramatically increased to 564.7 mg/g due to the special dual-doped architecture. Additional energy and electronic structure simulations showed that nearby NH^{3+} and SO^{2-} groups could produce frustrated Lewis pairs (FLPs). Due to improved electron transport between functional groups and Cr(VI) ions, such FLP-type sites can facilitate the adsorption and reduction of Cr(VI) ions. In order to effectively remove heavy metal ions, Chang et al. described the straightforward synthesis of N, S-co-doped carbon materials (NS–C) produced from PVC plastic wastes (HMIs).[23] Large specific surface area (1230 m^2/g) and strong heteroatom doping (4.55 at % N and 13.30 at % S) were two characteristics of the NS–C. The CDI electrode made with NS–C demonstrated excellent regeneration capability for the adsorption of a variety of low-concentration heavy metal ions, including Fe^{2+}, Co^{2+}, Ni^{2+}, Cu^{2+}, Pb^{2+}, and Cd^{2+}, as well as high removal efficiency (94–99 %) and high capacity (36–62 mg/L). The Awal group created a conjugate adsorbent that uses a two-step procedure to simultaneously detect and remove harmful Pb(II) ions.[24] Mesoporous silica was first created synthetically. In order to produce conjugate adsorbent utilizing the indirect doping technique, the surface of mesoporous silica was changed with ammonium (4-chloro-2-mercaptophenyl) carbamodithioate (ACMPC). The ACMPC ligand served as a molecular receptor that changed the signal when it connected with a Pb(II) ion at a particular pH level. When evaluating the sensitivity, selectivity, adsorption, and reusability, the use of certain functional organic ligands emphasizes the metal ions under specified conditions and minimizes experimental work. Based on the pH-dependent material, the Pb(II) ion was collected. Even after ACMPC was doped onto the mesoporous silica, the conjugate adsorbent still displayed high surface area and large pore volumes.

One approach to using magnetic nanoparticles for lead removal is to functionalize their surface with specific ligands or coatings that can selectively adsorb heavy metals such as lead. For example, nanoparticles coated with amine or carboxylic acid groups have been shown to adsorb lead ions effectively. The functionalized nanoparticles are dispersed in the wastewater, and a magnetic field is applied to separate the nanoparticles and the adsorbed lead from the water. The nanoparticles can be regenerated and reused for subsequent wastewater treatments. Dey et al. have introduced a novel nanomaterial called perylene diimide-coated magnetic nanoparticle for removing lead from contaminated water. The nanomaterial comprises perylene diimide functionalized with biocompatible amino acid (levodopa) coating the superparamagnetic Fe_3O_4 nanoparticle core. The nanomaterial used chelation between lead and L-DOPA of PDI to effectively remove lead with exceptionally high efficiency. The nanomaterial has a remarkable adsorption capacity of 1407.5 mg/g and a Kd value of 1.14×106 mL/g. It can effectively reduce the Pb(II) concentration from 4000 to 7 ppb with 99.97% efficiency, even at a low pH level.[25] Green cobalt-oxide nanoparticles (Co_3O_4 NPs) synthesized using chemical co-precipitation were used to remove Pb ions from simulated wastewater solutions. The NPs were characterized using various analytical techniques, including FTIR, Raman, SEM, UV visible, XRD, and BET. The maximum adsorption capacity of 450.45 mg/g was observed at 298.15 K, and 0.1 M HNO_3 and 0.1 M HCl were used to regenerate used Co_3O_4 NPs. The experimental data fit the Elovich rate equation better than the other three models. In addition, simulation results suggest that the Co atom in the Co_3O_4 NPs generates active delocalized surface states energetically favorable for Pb ion adsorption and removal.[26] The use of magnetic nanoparticles for lead removal offers several advantages, including high efficiency, low cost, and the potential for scale-up in large wastewater treatment plants. However, challenges such as particle aggregation, surface fouling, and potential toxicity of the nanoparticles must be addressed to implement this technology in real-world scenarios successfully.

Although many routes have been employed to produce heteroatom doped carbons that show considerable absorption capacity, they still depend on the time-consuming process and expensive harsh chemicals. Waste tires have been growing as a popular form of precursor for the development of carbon-based functional materials. Waste tires are rich in carbon content, and various trace impurities, such as sulfur, are removed in different gaseous forms during pyrolysis at low temperatures, which introduces varying degrees of porosity in the carbon framework.[27]

Considering these advantages, we report here the preparation of B doped porous carbon derived from the waste tire with low-temperature pyrolysis, followed by sodium borohydride treatment ($NaBH_4$) and evaluation of this material for Pb removal from wastewater.[28] The influence of different operating parameters such as contact time, temperature, and B concentration was investigated. The B doping exponentially increases the carbon adsorption capacity for lead removal from 32 to 98 %. This work may illuminate more fascinating ideas about heteroatom doped carbon as a high surface area adsorbent for refractory wastewater.

Experimental Section

Chemicals

Sodium borohydride ($NaBH_4$, 96 %, Sigma-Aldrich), melamine, boric acid (H_3BO_3, Alfa Aesar), urea (CH_4N_2O, Alfa Aesar) potassium hydroxide (KOH, ≥95 %, Sigma-Aldrich), ethanol (C_2H_5OH, ≥98 %, Sigma Aldrich), isopropanol (≥98 %, Sigma Aldrich). Milli-Q ultrapure water with resistance of 18 MΩ cm was used throughout this study.

Synthesis of g-Carbon-nitride sheets (g-C_3N_4)

2 g of melamine was pyrolyzed in an open atmosphere in a muffle furnace. An aluminum crucible containing melamine was subjected to the muffle furnace and increased the temperature of the furnace from room temperature to 550 °C with a ramping rate of 10 °C/min. The temperature was kept constant for 2 h and then allowed to cool down to room temperature.

Synthesis of B doped Carbon using boric acid

Initially the boric acid was mixed with melamine with a mortar and pestle with different ratios to make a homogenous solid mixture. The mixture was then subjected to furnace and repeated the above procedure to develop the B doped carbon.

Synthesis of B doped Carbon using sodium borohydride

$NaBH_4$ was mixed with the melamine with a mortar and pestle until the powder color change to dark brown, and then the crucible covered with the lid was subjected to muffle furnace, wherein the furnace temperature was increased from room temperature to 550 °C with a ramping rate of 10 °C/min. The temperature was kept constant for 2 h and then allowed to be cooled down to room temperature.

Activated Carbon derived from waste tire

A waste tire was used that contained no steel or synthetic cords. Before commencing the treatment process, the scrap tires were cut into 0.5 to 1 cm small pieces. After cutting, the waste tire pieces were put in a beaker filled with water and placed in a sonicator for about 30 minutes. After sonication, each piece was thoroughly washed with deionized water and washed with methanol and IPA afterward. These small pieces were then placed in an electric oven and heated to 100 °C to remove volatile content from the sample.

The waste tire samples were then placed in a crucible, and the furnace temperature was set to 550 °C with an increment of 10 °C/min. After 1 h, the samples were cooled to room temperature gradually within the furnace. After cooling down to room temperature, the carbon was obtained.

The activated carbon obtained from the waste tire was then mixed in a homogenous way with sodium borohydride, with the help of mortar and pestle, and was placed in the furnace for 1 h to be heated to a temperature of 550 °C to insert boron. After 1 h, the samples were cooled to room temperature gradually within the furnace. After cooling down to room temperature, B-doped activated carbon was obtained.

Results and Discussion

Predominantly, waste tires are particularly rich with carbon content (80 to 90 %) and are considered a mixture of elastomers (e.g., styrene, natural rubber, and butadiene).[27] The cross-linking molecular structure set in thermosetting nature makes its recycling more difficult. Thermal pyrolysis is considered an effective approach to recovering the maximum content of carbon (90 % by weight).[29] The thermal process generates non-condensable hydrocarbon gases that act as a nucleation site for the formation of a carbon frame. Researchers demonstrated that the B content in the carbon frame has a linear relation with the BH_4^- concentration. The hydride ions (H^-) released from $NaBH_4$ reveal a strong reducing ability that can act as an oxygen scavenger to generate oxygen defects and modify the structure.[30]

Raman spectroscopic analysis was performed to interrogate the molecular interactions, crystallinity, phases, and chemical structure of B-doped carbon. Figure 1a reveals two characteristic intense bands positioned at 1341 and 1598 cm^{-1} that correspond to the D band and the G band, respectively.[31] In general, the D line represents the disorder arrangement and defects of the carbon atom and appears from the Sp^2 hybridized carbon structure. The G band is associated with the E_2g mode vibration of sp^2-hybridized carbon and corresponds to the adjacent carbon atoms moving in a direction perpendicular to the plane of the graphitized sheets.[32] The intensity ratio of the D to G band (ID/IG) can be considered an important parameter to replicate the relative graphitization degree (atomic order degree) of the carbon structure. According to the

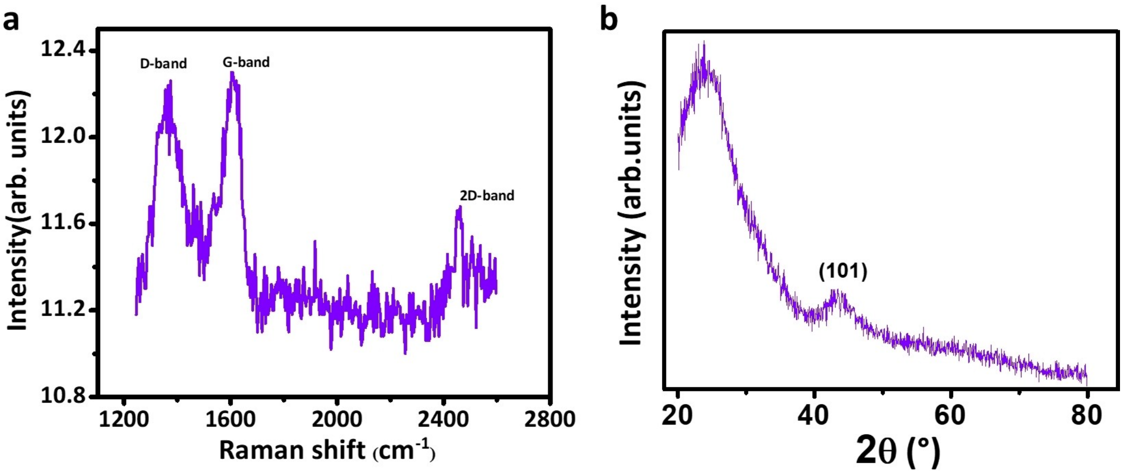

Figure 1. (a) Raman spectra and (b) XRD spectrum for B doped carbon derived from waste tire.

Ferrari and Robertson three-stage model, the ID/IG ratio demonstrates a different trend for graphitic and

amorphous carbon-based materials.[32] The relative intensity of the ID/IG value progressively increases with the enrichment of the graphitization degree. In our case, ID/IG ratio is observed to be 0.93 and corresponds to the activated carbon.[33] Moreover, the presence of a 2D band at ~2700 cm^{-1} (two phonons double resonance phenomenon) reveals the presence of a few layers of graphene oxide nanosheets.[34]

X-ray diffraction analysis (XRD) was implemented to investigate the phase purity and crystal structure of the synthesized material. Figure 1b shows the XRD spectrum of B doped carbon. The B doped carbon does not show any characteristic diffraction peak, which further confirms the amorphous structure of the material.[35] The structural flexibility allows the amorphous materials to regulate the exposed surface according to the reaction condition and provides a space for volume and surface-confined interactions. Amorphous materials have other unique surface self-healing features that enhance corrosion resistance and ensure structural stability in aggressive industrial wastewaters.[36] The high specific surface area and super-hydrophilicity accelerate the electrolyte diffusion kinetics, and these structural characteristics make the amorphous materials a selective candidate for heavy metals removal from wastewater.[36]

Scanning electron microscopy was performed to demonstrate the surface texture and morphology of the synthesized materials. Figure 2 reveals the SEM images recorded for B doped carbon and pristine carbon. From the SEM images, the highly layered and dense structures of the carbon can be noticed, which is probably due to interlayer stacking phenomena due to the electrostatic interaction between different functional groups anchored on the surface of the carbon.[31] The B addition altered the chemical structures, bonding pattern and decreases the oxophilicity of carbon, and decreases the surface stacking phenomena to the exposed more active center as an adsorption site for heavy metal removal.[37] The images further show that the sheets are uniform without any cluster agglomeration that is mostly observed for waste materials pyrolysis and decreases the effective contact portion between solid and liquids.

The synthesized material was also analyzed with the energy dispersive X-ray spectroscopy (EDS) to unveil the elemental composition (Figure 3). The spectrum reveals that the material is mainly composed of carbon and oxygen. The oxygen comes from the surface functionalization of carbon during the pyrolysis in an open atmosphere and its exposure to the environment.[38] A small trace quantity was observed for the impurities mainly for S, which is inherently present in the tire and cannot be 100 percent removed with washing.

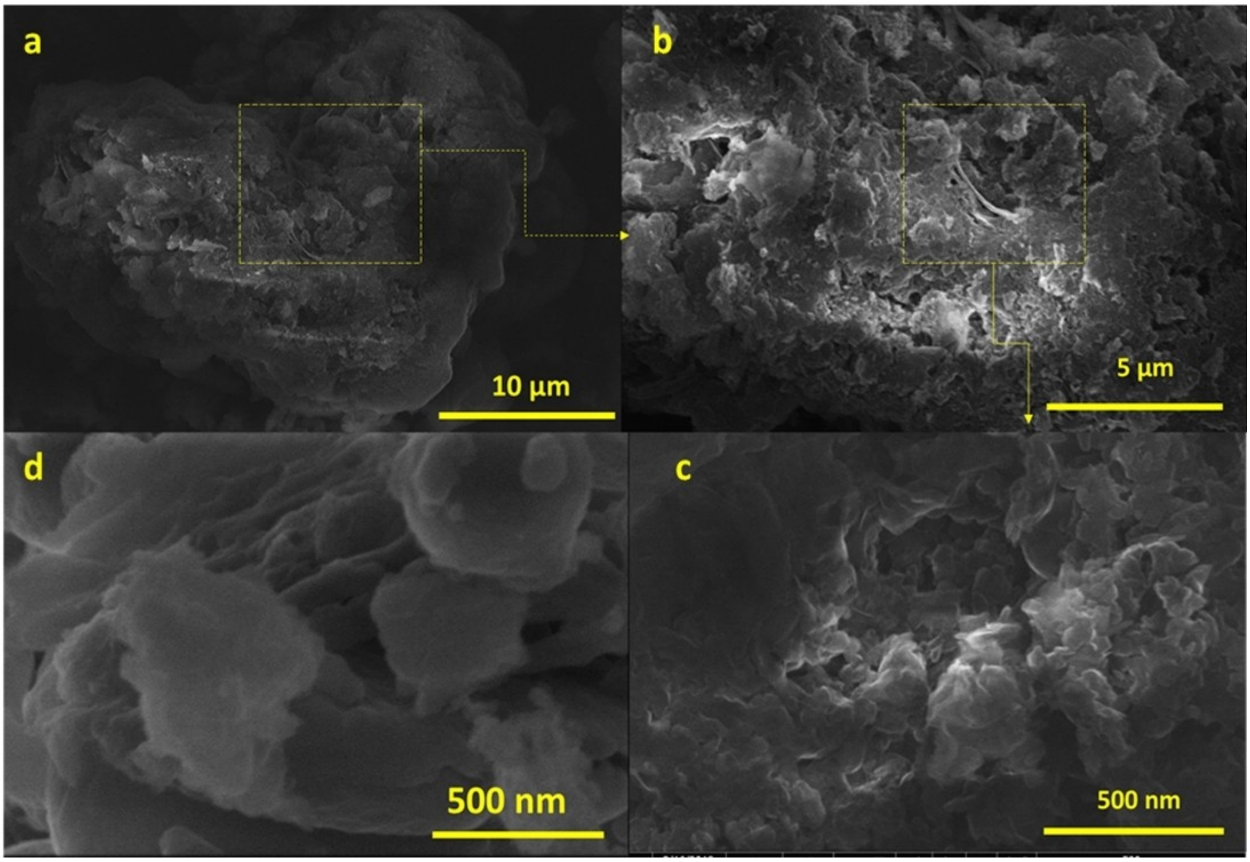

Figure 2. (a–c) SEM images of B doped carbon derived from waste tire, (d) Carbon synthesized from melamine.

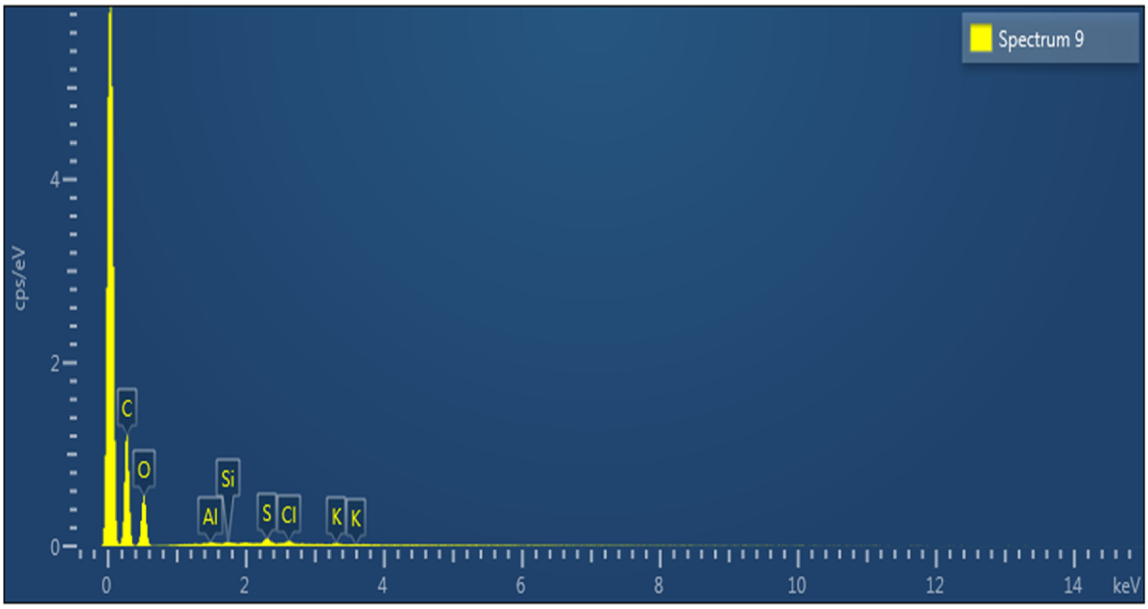

Figure 3. EDS spectrum for B doped carbon derived from waste tire.

The chemical environment, exact composition, and valance state of the synthesized catalyst were probed with X-ray photon spectroscopy (XPS), as depicted in Figure 4. The C 1s binding energy (BE = 284.5 eV) was used as an internal standard. The XPS spectrum demonstrated the existence of C, O, and B at the corresponding characteristic position. C 1s spectrum was deconvoluted using CASA-XPS software; high resolution spectrum reveals peaks at the BE of 284.5, 285.7, and 287.8 eV, corresponding to the C–C, C–O, O–C=O bonds, respectively.[39] The more intense peak at the BE of 284 eV unveiled that C is present mainly in SP2 form, providing both electron-dense and electrophilic centers to facilitate the heavy metal removal from contaminated water. The O 1s core-level spectrum shows two characteristic peaks at the BE of 528 and 531 eV.[40] The presence of these peaks validates the surface oxidation of carbon and enough oxidized groups are available on the carbon surface to reshuffle the electronic cloud and modulate the electronic structure according to the heterogeneous reaction conditions. The B 1s spectrum shows the characteristic peak at the BE of 187.9 eV, validating the successful doping of B in the carbon lattice structure.[41]

Interestingly, a considerable reduction was observed in the intensity of O after the B addition, demonstrating the reduction and B substitution phenomena. The B addition is thermodynamically favorable at high temperatures when an oxidized group is eliminated from the carbon, creating the oxygen vacancies and promoting the B addition.[42] The absence of a peak at the BE of 190 eV in the B 1s spectrum further confirms that B is substituted in elemental form.

B doped carbon activity for lead removal

The adsorption experiments were conducted by interacting 0.2 g of the samples with an 80 mL aqueous solution of lead (30 mg/L) at natural pH solution as shown in Figure 5. The experiments were performed in a round bottom flask subjected

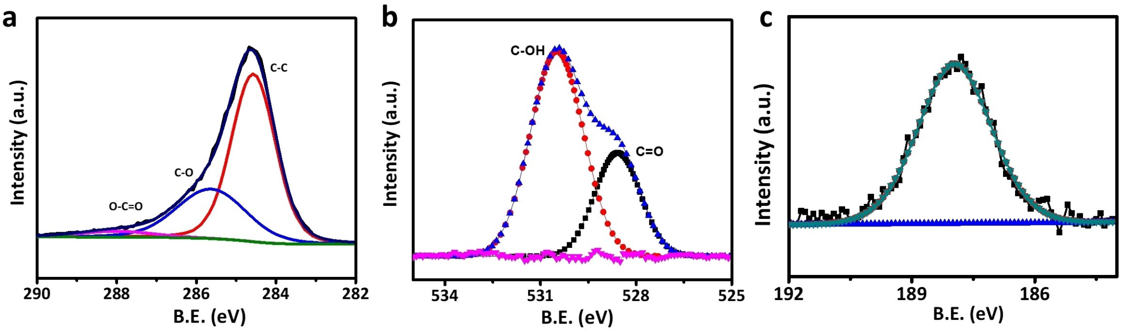

Figure 4. XPS core level spectra (a)C 1s, (b) O 1s, (c) B 1s.

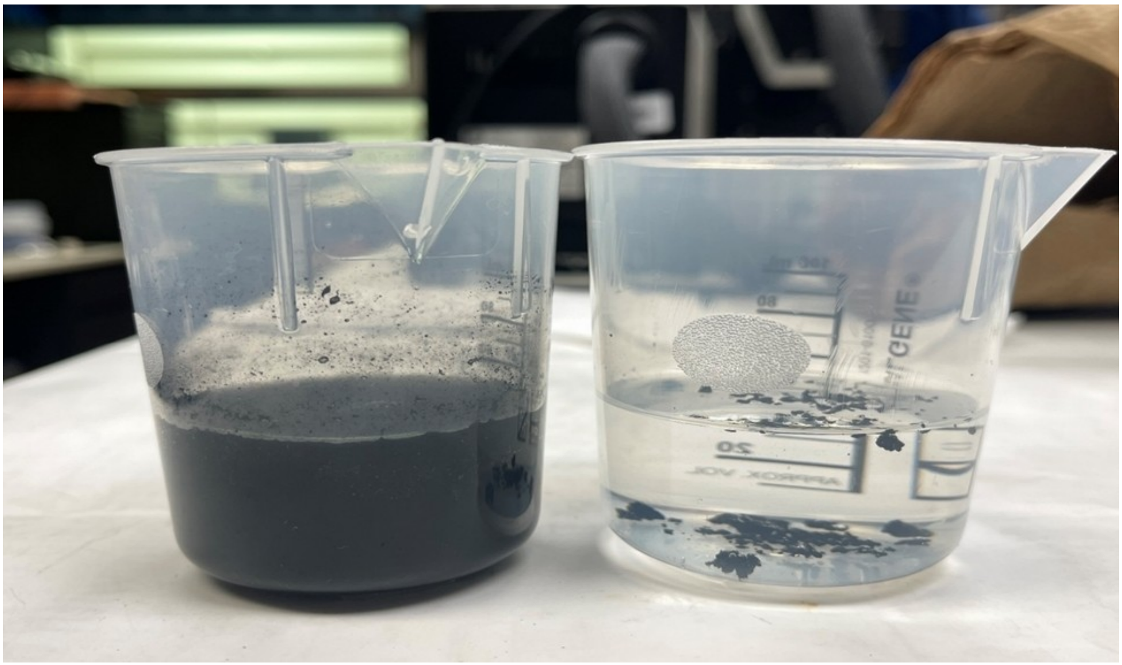

Figure 5. Left beaker is B-doped carbon obtained from waste tire treated with water containing lead, while right beaker has activated carbon obtained from waste tire treated with water containing lead.

to a thermal shaker for 1.5 h at 150 RPM.[43] The adsorbate and adsorbent were mixed at a homogenous rate to provide the maximum contact between solid and liquid, and to accelerate mass transfer. The remaining concentration of Pb in the solution was monitored by inductively coupled plasma optical emission spectroscopy (ICP-OES), after filtering the residue with Whatman filter paper to make the water carbon-free.[44] We have observed that the lead removal percentage (see Table 1) has a direct relation with the adsorbent dose, because it provides the maximum number of active sites for adsorption. Interestingly, the B doping exponentially increases the hydrophilicity of carbon and ensures the maximum contact between adsorbent and adsorbate. The B substation with the surface carbon changed the chemical structure and coordination of carbon, reshuffles the electronic population, and increases the orbital compatibility between active centers and lead ions.[45] ICP-OES results demonstrated that the B introduction increases the lead removal efficiency from 30 to 98 %. Interestingly this maximum efficiency was observed with a low mass of adsorbent i.e., 2 g/L which reveals the economic viability of the adsorbent for lead removal.

For the chemisorption of potentially harmful metals, the % removal effectiveness of B-doped carbon is directly related to the pH of the medium. Therefore, the influence of pH (2–12) on (Pb-II) adsorption by synthesized material was studied using a 1 g mass of adsorbent for 20 minutes of reaction time. Figure 6A that increasing the pH of the heterogeneous solution increased metal removal efficiency, achieving maximum removal efficiency (> 98%) at pH 8. After that, changing the pH from 8 to 12 did not affect metal removal efficiency, demonstrating the constant adsorption behavior. The mass of the substrate also has a critical role in the percentage absorption efficiency. We have used the different masses of the designed material to evaluate the relationship between mass dosage and removal efficiency. The experimental results demonstrated the direct relationship between mass dosage and removal efficiency. However, the 99 % removal efficiency of Pb removal with a small dosage of 1 g revealed the commercial interest of the fabricated material (Figure 6B). The contact time was also optimized by performing the reaction at different intervals. Due to the excellent hydrophilic character of the fabricated material, the catalyst revealed maximum removal performance with a short exposure time of 15 minutes. (Figure 6C)

SEM images of B-doped carbon derived from melamine can reveal the morphology and microstructure of the material, including any contamination or impurities present. The SEM

Table 1. ICP-OES analysis to compare the efficiency of B-doped activated carbon with activated carbon.

No.	Sample	Initial Pb concentration (mg/L)	Final Pb concentration (mg/L)	Efficiency (%)
	Standard Solution	33.695	33.695	Null
1	Simple activated carbon	33.695	26.132	22.45
2	B-doped activated carbon	33.695	0.666	98.02

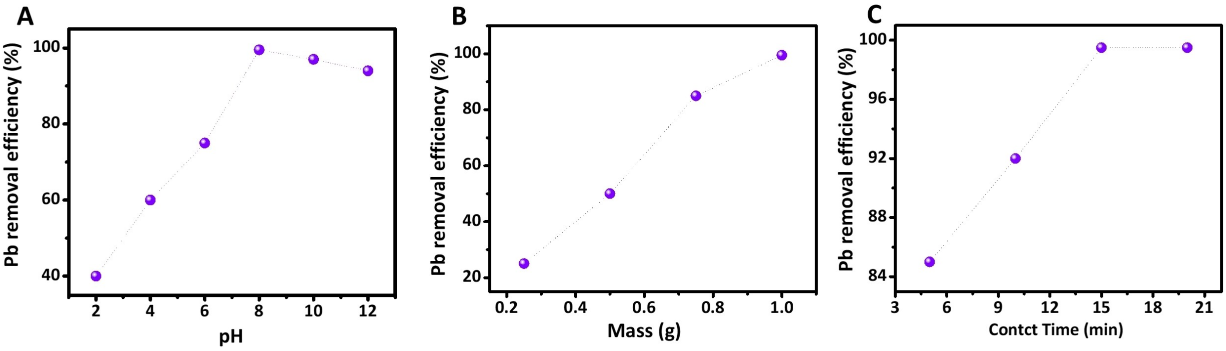

Figure 6. Pb removal efficiency in different experimental conditions. (a) at different pH of solution, (b) using different mass of designed material and (c) different contact time at solid liquid interface.

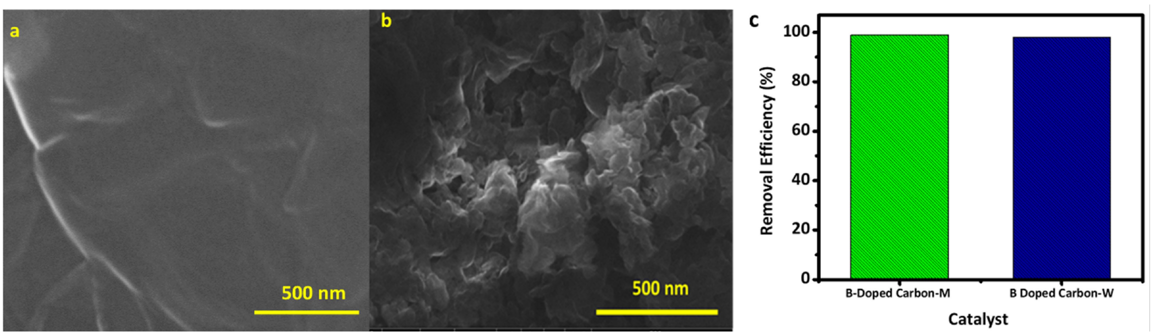

Figure 7. SEM images of B doped carbon (a) Derived from melamine, and (b) derived from waste carbon. (c) Pb removal efficiency of B doped carbon derived from melamine and waste carbon.

images of B-doped carbon derived from melamine show a sheet-like morphology without contamination, suggesting that the material is highly pure and well-defined (Figure 7 a and b). The sheet-like morphology typically indicates that the material comprises thin, flat layers stacked on each other. The absence of contamination in the SEM image means the controlled synthesis of B-doped carbon. The B-doped carbon derived from melamine and waste carbon was explored to evaluate the removal efficiency of both materials. However, the removal efficiency is slightly higher for the carbon derived from the melamine, most likely due to the high specific surface area without any surface contaminations. However, the negligible difference in the efficiency difference with a removal efficiency of around 98%, demonstrated the practical viability of our material for Pb removal from the wastewater (Figure 7c).

Conclusion

In summary, we have fabricated B-doped carbon derived from waste tires using a facile and scalable pyrolysis approach to meet the industrial demands of adsorbents for heavy metals removal from wastewater. Its hydrophilicity, disorder structure, and many adsorption sites with high absorption capacity ensure the maximum removal of heavy metals from wastewater. The physical characterization validates the successful incorporation of B in the carbon structure and alters the electronic structure without disturbing the surface structure. The ICP-OES analysis demonstrated that B insertion exponentially enhanced the capturing efficiency of adsorbent for lead removal. We suppose this work opens a new endeavor to design robust, cost-effective adsorbent material for heavy metal removal from wastewater.

Acknowledgements

The author would like to acknowledge the College of Engineering – Texas A &M University-Kingsville.

Conflict of Interest

The authors declare no conflict of interest.

Data Availability Statement

The data that support the findings of this study are available from the corresponding author upon reasonable request.

Keywords: adsorption · B doped porous carbon · lead · tire waste · wastewater treatment

[1] R. Jalali, H. Ghafourian, Y. Asef, S. J. Davarpanah, S. Sepehr, *J. Hazard. Mater.* **2002**, *92*, DOI 10.1016/S0304-3894(02)00021-3.

[2] V. K. Gupta, M. Gupta, S. Sharma, *Water Res.* **2001**, *35*, 1125–1134.

[3] K. Conrad, H. C. Bruun Hansen, *Bioresour. Technol.* **2007**, *98*, 89–97, DOI 10.1016/j.biortech.2005.11.018.

[4] K. M. Ibrahim, T. Akashah, *Environ. Geol.* **2004**, *46*, 865–870.

[5] M. M. Husein, J. H. Vera, M. E. Weber, *Sep. Sci. Technol.* **1998**, *33*, 1889–1904 DOI 10.1080/01496399808545911.

[6] S. W. Lin, R. M. F. Navarro, *Chemosphere* **1999**, *39*, 1809–1817, DOI 10.1016/S0045-6535(99)00074-0.

[7] D. Petruzzelli, M. Pagano, G. Tiravanti, R. Passino, *Solvent Extr. Ion Exch.* **1999**, *17*, 677–694, DOI 10.1080/07366299908934633.

[8] A. Saeed, M. Iqbal, M. W. Akhtar, *J. Hazard. Mater.* **2005**, *117*, 65–73, DOI 10.1016/j.jhazmat.2004.09.008.

[9] S. Doyurum, A. Çelik, *J. Hazard. Mater.* **2006**, *138*, 22–28.

[10] C. P. Dwivedi, J. N. Sahu, C. R. Mohanty, B. R. Mohan, B. C. Meikap, *J. Hazard. Mater.* **2008**, *156*, 596–603, DOI 10.1016/j.jhazmat.2007.12.097.

[11] C. K. Singh, J. N. Sahu, K. K. Mahalik, C. R. Mohanty, B. R. Mohan, B. C. Meikap, *J. Hazard. Mater.* **2008**, *153*, 221–228, DOI 10.1016/j.jhazmat.2007.08.043.

[12] J. N. Sahu, S. Agarwal, B. C. Meikap, M. N. Biswas, *J. Hazard. Mater.* **2009**, *161*, 317–324, DOI 10.1016/j.jhazmat.2008.03.094.

[13] S. Candamano, A. Policicchio, G. Conte, R. Abarca, C. Algieri, S. Chakraborty, S. Curcio, V. Calabrò, F. Crea, R. G. Agostino, *J. Cleaner Prod.* **2022**, *330*, 129843, DOI 10.1016/j.jclepro.2021.129843.

[14] M. Suzuki, *Carbon N. Y.* **1994**, *32*, 577–586, DOI 10.1016/0008-6223(94)-90075-2.

[15] S. I. El-Hout, S. Y. Attia, S. G. Mohamed, S. M. Abdelbasir, *J. Environ. Manage.* **2022**, *304*, 114222, DOI 10.1016/j.jenvman.2021.114222.

[16] J. Jjagwe, P. W. Olupot, E. Menya, H. M. Kalibbala, *J. Bioresour. Bioprod.* **2021**, *6*, 292–322, DOI 10.1016/j.jobab.2021.03.003.

[17] H. Yi, K. Nakabayashi, S. H. Yoon, J. Miyawaki, *Carbon N. Y.* **2021**, *183*, 735–742, DOI 10.1016/j.carbon.2021.07.061.

[18] Y. Gao, Q. Yue, B. Gao, A. Li, *Sci. Total Environ.* **2020**, *746*, 141094, DOI 10.1016/j.scitotenv.2020.141094.

[19] Z. Heidarinejad, M. H. Dehghani, M. Heidari, G. Javedan, I. Ali, M. Sillanpää, *Environ. Chem. Lett.* **2020**, *18*, 393–415, DOI 10.1007/s10311-019-00955-0.

[20] Q. Abbas, R. Raza, I. Shabbir, A. G. Olabi, *J. Sci. Adv. Mater. Devices* **2019**, *4*, 341–352, DOI 10.1016/j.jsamd.2019.07.007.

[21] A. Munir, T. ul Haq, I. Hussain, A. Qurashi, U. Ullah, M. J. Iqbal, I. Hussain, *ChemSusChem* **2019**, *12*, 5117–5125, DOI 10.1002/cssc.201902505.

[22] J. Chen, M. Yuan, W. Cai, J. Wei, J. Zhou, P. Liu, Z. Yang, J. Luo, Q. Xia, Z. Cai, *Chem. Eng. J.* **2021**, *422*, 130153, DOI 10.1016/j.cej.2021.130153.

[23] Y. Chang, Q. Dang, I. Samo, Y. Li, X. Li, G. Zhang, Z. Chang, *RSC Adv.* **2020**, *10*, 4064–4070, DOI 10.1039/c9ra09237d.

[24] M. R. Awual, *Chem. Eng. J.* **2016**, *289*, 65–73, DOI 10.1016/j.cej.2015.12.078.

[25] S. Dey, S. Mahanty, A. Saha, P. Kumar, R. Saha, C. Kar, P. Chaudhuri, P. K. Sukul, *Mater. Adv.* **2020**, *1*, 1817-1828, DOI 10.1039/d0ma00477d.

[26] S. Singh, P. N. T. S. S. K. Naik, U. Basavaraju, C. Thamaraiselvan, S. K. Behera, R. Kour, P. Dwivedi, S. Subramanian, N. A. Khan, J. Singh, P. C. Ramamurthy, *Environ. Res.* **2023**, *222*, 115335.

[27] J. D. Martínez, N. Cardona-Uribe, R. Murillo, T. García, J. M. López, *Waste Manage.* **2019**, *85*, 574–584, DOI 10.1016/j.wasman.2019.01.016.

[28] T. Ul Haq, M. Pasha, Y. Tong, S. A. Mansour, Y. Haik, *Appl. Catal. B* **2021**, *301*, 120836.

[29] M. Niu, R. Sun, K. Ding, H. Gu, X. Cui, L. Wang, J. Hu, *Energy* **2022**, *240*, 122808, DOI 10.1016/j.energy.2021.122808.

[30] T. ul Haq, Y. Haik, Y. Bicer, A. Munir, S. Mansour, *ChemCatChem* **2020**, *12*, 3585–3597, DOI 10.1002/cctc.202000392.

[31] A. Munir, T. U. Haq, A. Qurashi, H. U. Rehman, A. Ul-Hamid, I. Hussain, *ACS Appl. Energy Mater.* **2019**, *2*, 363–371.

[32] S. S. Gunasekaran, S. K. Elumalali, T. K. Kumaresan, R. Meganathan, A. Ashok, V. Pawar, K. Vediappan, G. Ramasamy, S. Z. Karazhanov, K. Raman, R. Subashchandra Bose, *Mater. Lett.* **2018**, *218*, 165–168, DOI 10.1016/j.matlet.2018.01.172.

[33] Z. Wei, R. Pan, Y. Hou, Y. Yang, Y. Liu, *Sci. Rep.* **2015**, *5*, 15664, DOI 10.1038/srep15664.

[34] G. K. Gupta, P. Sagar, S. K. Pandey, M. Srivastava, A. K. Singh, J. Singh, A. Srivastava, S. K. Srivastava, A. Srivastava, *Nanoscale Res. Lett.* **2021**, *16*, 85, DOI 10.1186/s11671-021-03545-8.

[35] T. ul Haq, S. Mansour, Y. Haik, *ACS Appl. Mater. Interfaces* **2022**, *14*, 20443–20454, DOI 10.1021/acsami.1c24304.

[36] T. ul Haq, Y. Haik, *Catal. Today* **2021**, *400–401*, 14–25, DOI 10.1016/j.cattod.2021.09.015.

[37] Y. Liu, Y. Xiong, P. Xu, Y. Pang, C. Du, *Sci. Total Environ.* **2020**, *708*, 134918, DOI 10.1016/j.scitotenv.2019.134918.

[38] M. Sabet, K. Mahdavi, *Appl. Surf. Sci.* **2019**, *463*, 283–291, DOI 10.1016/j.apsusc.2018.08.223.

[39] A. Munir, T. Haq, M. Saleem, A. Qurashi, S. Z. Hussain, F. Sher, A. Jilani, I. Hussain, *Electrochim. Acta* **2020**, *341*, 136032.

[40] D. Shrestha, S. Maensiri, U. Wongpratat, S. W. Lee, A. R. Nyachhyon, *J. Environ. Chem. Eng.* **2019**, *7*, 103227, DOI 10.1016/j.jece.2019.103227.

[41] K. Ranganathan, A. Morais, I. Nongwe, C. Longo, A. F. Nogueira, N. J. Coville, *J. Mol. Catal. A* **2016**, *422*, 165–174, DOI 10.1016/j.molcata.2015.10.024.

[42] T. U. Haq, Y. Haik, I. Hussain, H. U. Rehman, T. A. Al-Ansari, *ACS Appl. Mater. Interfaces* **2021**, *13*, 468–479.

[43] J. Acharya, J. N. Sahu, C. R. Mohanty, B. C. Meikap, *Chem. Eng. J.* **2009**, *149*, 249–262, DOI 10.1016/j.cej.2008.10.029.

[44] J. N. Sahu, J. Acharya, B. K. Sahoo, B. C. Meikap, *Desalin. Water Treat.* **2016**, *57*, 2016–2017, DOI 10.1080/19443994.2014.979446.

[45] H. Zhou, S. Wu, Y. Zhou, Y. Yang, J. Zhang, L. Luo, X. Duan, S. Wang, L. Wang, D. C. W. Tsang, *Environ. Int.* **2019**, *128*, 77–88, DOI 10.1016/j.envint.2019.04.006.

Submitted: November 13, 2022
Accepted: March 23, 2023